PRESENTED AT ICAS 2008
ANCHORAGE, ALASKA SEPTEMBER 2008

NONLINEAR AEROELASTICITY OF CURRENT AND FUTURE AEROSPACE VEHICLES

Earl Dowell, Kenneth Hall, Robert Kielb, Deman Tang, and Jeffrey Thomas
Duke University
Charles Denegri, Jr., U.S. Air Force, SEEK EAGLE Office

FUNDAMENTAL FSI/AEROELASTIC ISSUES OF LARGE SCALE AIRCRAFT

- ***THE PHYSICAL PHENOMENA OF INTEREST***

WING/STORES FLUTTER/LCO OF FIGHTER AIRCRAFT

WING ROCK/LCO and ABRUPT WING STALL OF FIGHTER AIRCRAFT

FLUTTER/LCO OF HIGH ALTITUDE LONG ENDURANCE (HALE) LARGE SPAN, HIGHLY FLEXIBLE AIRCRAFT

PANEL FLUTTER/LCO OF SUPERSONIC/HYPERSONIC AIRCRAFT

- ***FOR A BETTER UNDERSTANDING OF THESE PHYSICAL PHENOMENA, A NONLINEAR MODEL OF THE FLUID AND/OR STRUCTURE IS REQUIRED.***

REFERENCES

1. E. H. Dowell, "Aeroelasticity of Plates and Shells," Kluwer Academic, Norwell, MA, 1975.
2. P. P. Friedmann, "Renaissance of Aeroelasticity and Its Future, " Journal of Aircraft, Vol. 36, January-February 1999, pp. 105-121.
3. E. H. Dowell and K.C. Hall, "Modeling of Fluid-Structure Interaction," Annual Review of Fluid Mechanics, Vol. 33, 2001, pp. 445-490.
4. E. H. Dowell and D. M. Tang, "Nonlinear Aeroelasticity and Unsteady Aerodynamics," AIAA Journal, Vol. 40, September 2002, pp. 1697-1707.
5. D. J. Lucia and P. S. Beran, "Projection Methods for Reduced Order Models of Compressible Flows," Journal of Computational Physics, Vol. 188, June 10 2003, pp. 252-280.
6. E. Dowell, J. Edwards and T. Straganac, "Nonlinear Aeroelasticity," Journal of Aircraft, September-October, 2003, pp. 857-874. An electronic bibliography with nearly a 1000 items is available upon request from the first author.
7. P. S. Beran, D. J. Lucia and C. L. Pettit, "Reduced-Order Modeling of Limit-Cycle Oscillation for Aeroelastic Systems," Journal of Fluids and Structures, Vol. 19, June 2004, pp. 575-590.
8. D. J. Lucia, P. S. Beran and W. A. Silva, "Aeroelastic System Development Using Proper Orthogonal Decomposition and Volterra Theory," Journal of Aircraft, , Vol. 42, March-April, 2005, pp 509-518.
9. R. M. Hall, S. H. Woodson and J. R. Chambers, "Accomplishments of the Abrupt Wing Stall Program," Journal of Aircraft, May-June 2005, pp. 653-660.
10. G. H. Parker, R. C. Maple and P. S. Beran, "Computational Aeroelastic Analysis of Store-Induced Limit-Cycle-Oscillation," Journal of Aircraft, Vol. 44, January-February 2007, pp. 48-59.
11. J. Dugundji, "Some Aeroelastic and Nonlinear Vibration Problems Encountered on the Journey to Ithaca," AIAA Journal, Vol. 46, No. 1, January 2008, pp. 21-35.

REFERENCES cont'd

12. J.J. McNamara and P.P. Friedmann, "Aeroelastic and Aerothermoelastic Analysis of Hypersonic Vehicles: Current Status and Future Trends," AIAA Paper 2007-2013, Presented at the 48th AIAA/ASME/ASCE/AHS/ASC Structures, Structural Dynamics, and Materials Conference, 23-26 April 2007, Honolulu, HA.
13. NATO RTO SYMPOSIA, LOEN, NORWAY, MAY 5-8,2008, LIMIT CYCLE OSCILLATIONS AND OTHER AMPLITUDE - LIMITED, SELF-EXCITED OSCILLATIONS (of fluid-structural systems) ADVANCED METHODS IN AEROELASTICITY
14. W. Shyy, Y. Lian, J. Tang, and D. Viiera, "Aerodynamics of Low Reynolds Number Flyers," Cambridge University Press, 2007.
15. J.P. Thomas, E.H. Dowell, and K.C. Hall, "Using Automatic Differentiation to Create a Nonlinear Reduced Order Model Aeroelastic Solver," AIAA Paper 2008-2322, 49th AIAA/ASME/ASCE/AHS/ASC Structures, Structural Dynamics and Materials (SDM) Conference, Schaumburg, IL, April 2008.
16. D.M. Tang and E.H. Dowell, "Experimental and Theoretical Study on Flutter and Limit Cycle Oscillations of High-Aspect-Ratio Wings," AIAA journal, Vol. 39, No. 8, 2001, pp. 1430-1441.
D.M. Tang and E.H. Dowell, "Experimental and Theoretical study of Gust Response for a High-Aspect-Ratio Wing," AIAA Journal, Vol. 40, No. 3, 2002, pp. 419-429.
18. D.M. Tang and E.H. Dowell, "Limit-Cycle Hysteresis Response for a High-Aspect-Ratio Wing Model," Journal of Aircraft, Vol. 39, No. 5, September-October 2002, pp. 885-888.

NONLINEAR AEROELASTIC PHENOMENA ARE NOT NEW!

- ***STALL FLUTTER (TURBOMACHINERY and ROTORCRAFT BLADES)***

SEPARATED FLOWS **THAT LEAD TO FLUTTER AND LCO HAVE BEEN STUDIED FOR MANY YEARS OFTEN USING EMPIRICAL AND HIGHLY SIMPLIFIED AERODYNAMIC (FLUID) MODELS. HOWEVER, MORE RECENT WORK USES COMPUTATIONAL FLUID DYNAMIC/STRUCTURAL DYNAMIC (CFD/CSD) MODELS.**

SEPARATED FLOW **IS THOUGHT TO BE IMPORTANT FOR THE F-16 LCO AS WELL.**

- ***PANEL FLUTTER (THIN SKINS OF HIGH SPEED VEHICLES)***

EARLY MAJOR DIFFERENCES BETWEEN THEORY AND EXPERIMENT WERE EVENTUALLY RESOLVED WHEN IT WAS REALIZED THAT ***STRUCTURAL NONLINEARITIES ARE ESSENTIAL*****TO UNDERSTANDING THE PHYSICAL PHENOMENA. THE FIRST REPORTED INSTANCE OF PANEL FLUTTER WAS ON THE V-2 ROCKET OF WW II.**

- ***ROTORCRAFT BLADE FLUTTER (AEROMECHANICAL INSTABILITY)***

BECAUSE LARGE DEFORMATIONS OF THE STRUCTURE OCCUR PRIOR TO THE ONSET OF THE DYNAMIC INSTABILITY, A ***NONLINEAR STRUCTURAL MODEL IS ESSENTIAL*** **TO PREDICTING EVEN THE ONSET OF THE DYNAMIC INSTABILITY. THIS WORK DATES TO THE DESIGN OF HINGELESS ROTORS IN THE 1970s.**

HALE AIRCRAFT **HAVE SIMILAR STRUCTURAL AND FLUID (?) NONLINEAR BEHAVIOR**

NEITHER ARE NONLINEAR FLUID INSTABILITY PHENOMENA NEW!

- **HYDRODYNAMIC INSTABILITY OF LAMINAR FLOWS LEADS (EVENTUALLY) TO TURBULENCE**

FROM A DYNAMICS PERSPECTIVE, ***TURBULENCE IS A VERY COMPLEX LIMIT CYCLE OSCILLATION DUE TO A HOPF BIFURCATION (FLUTTER).***

- **ABRUPT WING STALL MAY BE A** ***LARGE SCALE INSTABILITY OF A SEPARATED FLOW***

WHAT IS NEW?

- ***COMPUTATIONAL MODELS HAVE BEEN DEVELOPED THAT ARE OF HIGHER PHYSICAL FIDELITY and WITH EVER FASTER SOLUTION METHODS.***

NAVIER-STOKES FLUID MODELS AND NONLINEAR ELASTIC STRUCTURAL MODELS ARE NOW WIDELY AVAILABLE. BUT ARE THEY USEABLE?

REDUCED ORDER MODELS

MODAL MODELS FOR THE FLUID AND STRUCTURE (Eigenmodes, Proper Orthogonal Decomposition)

PERIODICITY IN TIME (Harmonic Balance Methods)

LINEAR AND NONLINEAR TRANSFER FUNCTIONS (Volterra Series)

- ***A MORE SUBSTANTIAL WIND TUNNEL AND FLIGHT TEST DATA BASE IS AVAILABLE***

F-16 FLIGHT TESTS (SEEK EAGLE OFFICE, EGLIN AFB)

HALE WING WIND TUNNEL TESTS (DUKE UNIVERSITY)

AIRFOILS AND WINGS WITH FREEPLAY WIND TUNNEL TESTS (DUKE UNIVERSITY, ONERA)

TRANSONIC AEROELASTIC WIND TUNNEL TESTS (NASA LANGLEY RESEARCH CENTER, DLR GOTTINGEN, NLR AMSTERDAM)

ABRUPT WING STALL WIND TUNNEL AND FLIGHT TESTS (NASA LANGLEY RESEARCH CENTER, NAVY)

WHAT ARE THE KEY RESEARCH QUESTION AND ISSUES?

- **WHAT ARE THE *FUNDAMENTAL* PHYSICAL PHENOMENA OF INTEREST?**

  FLUTTER (LINEAR INSTABILITY OF FLUID-STRUCTURAL SYSTEMS)

  LIMIT CYCLE OSCILLATIONS (NONLINEAR OSCILLATIONS OF FLUID-STRUCTURAL SYSTEMS)

  DYNAMICS OF SEPARATED FLOWS

  DYNAMICS OF THE INTERACTION BETWEEN OSCILLATING SHOCK WAVES AND SEPARATED FLOWS

- **IS THERE AN ADEQUATE DATA BASE OF EXPERIMENTAL RESULTS TO UNDERSTAND THESE PHENOMENA AND EVALUATE THEORETICAL/COMPUTATIONAL MODELS?**

- **HOW WELL DO CURRENT THEORETICAL/COMPUTATIONAL MODELS DESCRIBE THESE PHENOMENA EITHER FOR GAINING FUNDAMENTAL UNDERSTANDING OR FOR DESIGN?**

TABLE I

THE FOLLOWING SIX VIDEOS ARE FOR THE HALE WING, THE F-16 AIRCRAFT, AND A FOLDING WING, RESPECTIVELY.

- VIDEO #1 IS A VIDEO FROM A COMPUTATIONAL SIMULATION OF A NONLINEAR AEROELASTIC MODEL OF THE *HALE WING* THAT IS BASED UPON
  (1) A LARGE AMPLITUDE NONLINEAR STRUCTURAL MODEL
  AND
  (2) A NONLINEAR AERODYNAMIC (ONERA) MODEL THAT INCLUDES THE EFFECTS OF FLOW SEPARATION

- VIDEO # 2 IS A VIDEO OF THE WIND TUNNEL TEST OF AN AEROELASTIC MODEL OF THE *HALE WING*

  NOTE THE COMPUTATIONAL SIMULATION AND THE WIND TUNNELTEST BOTH SHOW THE SAME LCO PHENOMENA.

- VIDEO #3 IS A VIDEO FROM A COMPUTATIONAL SIMULATION OF A NONLINEAR AEROELASTIC MODEL OF AN F-16 CONFIGURATION THAT IS BASED UPON
  (1) A NONLINEAR NAVIER-STOKES AERODYNAMIC MODEL AND
  (2) A LINEAR STRUCTURAL MODEL.
  THE INSET SHOWS THE LCO AMPLITUDE AT THE WING TIP PLOTTED VERSUS MACH NUMBER. THE VIDEO PER SE SHOWS THE STRUCTURAL MOTION OF THE ENTIRE WING AT THREE DIFFERENT MACH NUMBERS LABELED AS POINTS 1, 2 AND 3. NOTE THAT THE STRUCTURAL NODE LINES ARE MOVING DURING THE LCO AS INDICATED BY THE LIGHT AND DARK SHADING.

- VIDEO #4 IS A VIDEO FROM THE SAME COMPUTATIONAL SIMULATION, BUT NOW SHOWING AN END-ON VIEW OF THE WING TIP AND ALSO SHOWING THE FLOW FIELD IN TERMS OF MACH NUMBER CONTOURS. THE SHOCK IN THE FLOW AND THE TRAILING EDGE SEPARATION ARE VISIBLE IN THE VIDEO. NOTE THE STRUCTURAL MOTION IN THIS VIDEO IS THE ACTUAL SIZE WHILE IN VIDEO #3 THE STRUCTURAL MOTION HAS BEEN MAGNIFIED FOR EASIER VIEWING.

- VIDEO #5 TOP VIEW OF FOLDING WING FLUTTER AND LCO WIND TUNNEL TEST.

- VIDEO #6 END VIEW …….

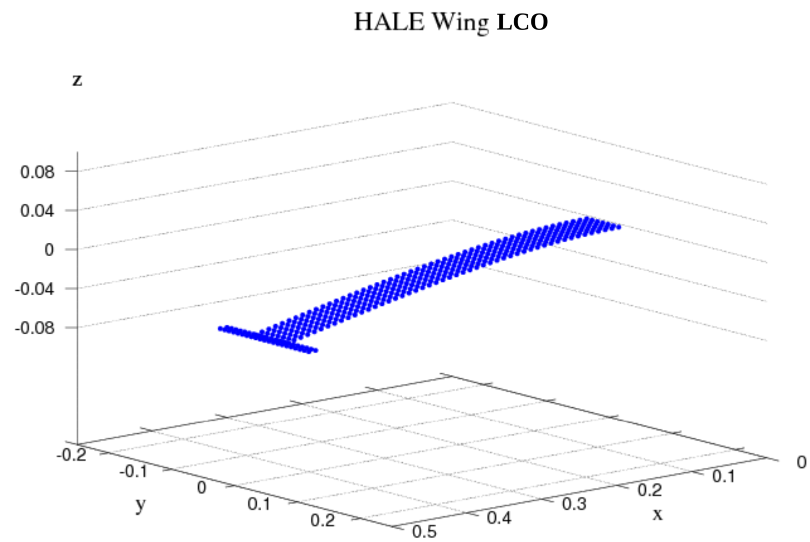

- FIGURE 1: Hale Simulations: Front View

HALE WING LCO

- FIGURE 2: Hale Experiments: Front View

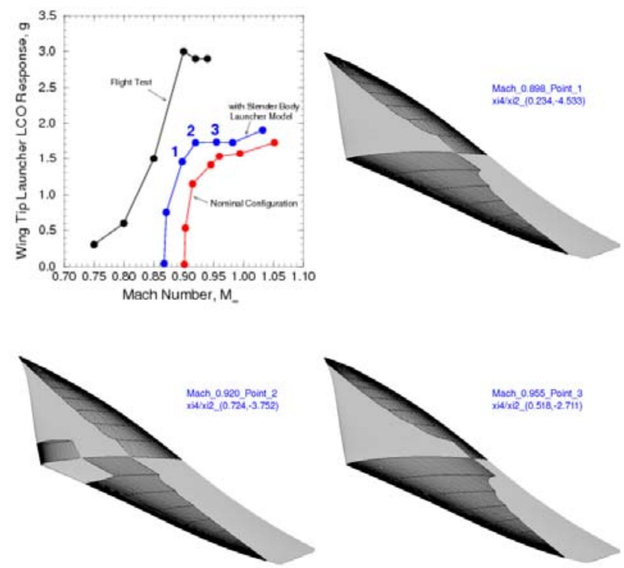

• FIGURE 3: F-16 LCO

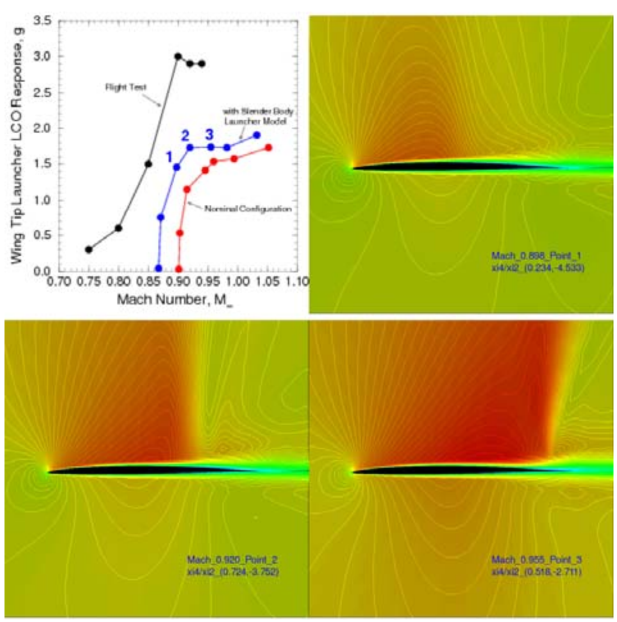

• FIGURE 4: F-16 LCO

FOLDING WING LCO

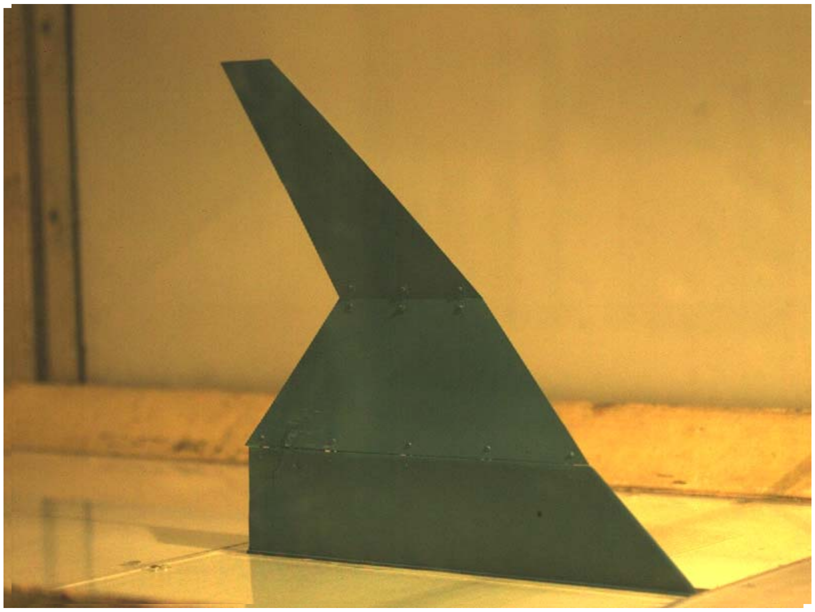

- FIGURE 5

FOLDING WING LCO

- FIGURE 6

SCHEMATIC OF LIMIT CYCLE OSCILLATION RESPONSE

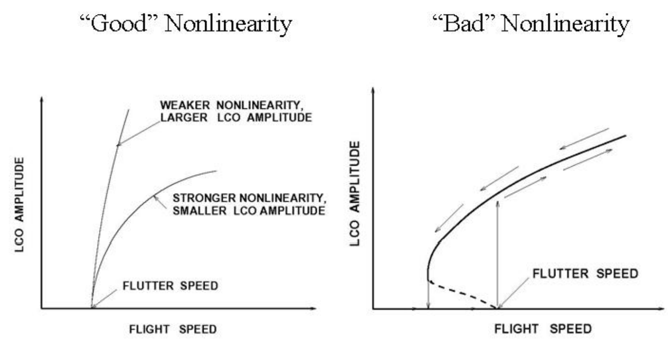

- FIGURE 7

LCO AMPLITUDE VS. FLOW VELOCITY

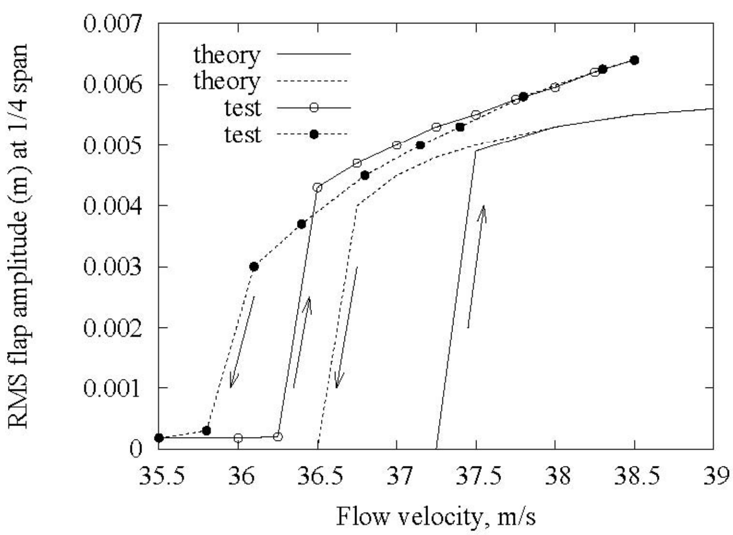

- FIGURE 8 **HALE WING LCO**

LCO FREQUENCY VS. FLOW VELOCITY

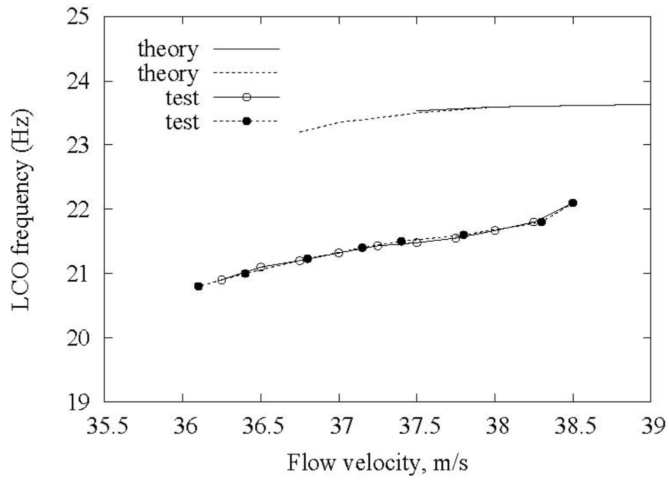

- FIGURE 9 **HALE WING LCO**

THE SEVERAL PHYSICAL SOURCES OF NONLINEARITIES

STRUCTURE

- CONTROL SURFACE FREE-PLAY (SUBCRITICAL & VERY STRONG)
- WING-STORE FREE-PLAY (?)
- PLATE-LIKE STIFFNESS (SUPERCRITICAL & STRONG)
- VERY HIGH ASPECT RATIO WING (SUBCRITICAL & MODERATELY STRONG)

FLUID (OUR FOCUS TODAY)

- SHOCKWAVES (SUB OR SUPERCRITICAL & WEAK USUALLY, BUT MAY BE STRONG)
- SEPARATED FLOW (SUB OR SUPERCRITICAL & STRONGER)

- FIGURE 10

F-16 Forward Wingtip Launcher Accelerometer LCO Response Trend (Denegri and Dubben (2003))

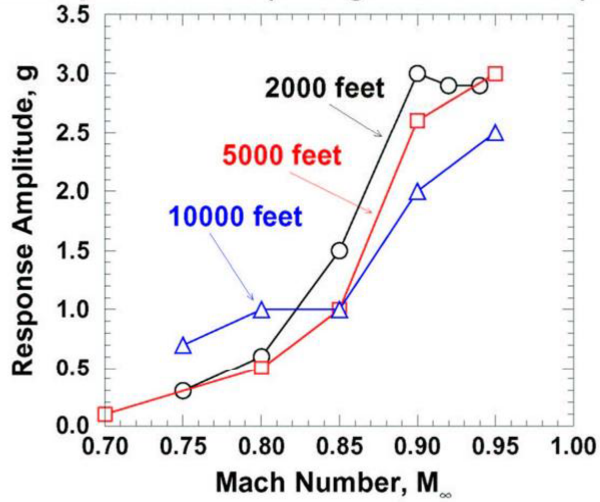

- FIGURE 11 **F-16 LCO**

Sample F-16 NASTRAN Structural Model Mode Shapes

Modes 2 and 4 Dominate Flutter Onset and LCO As Will Be Shown Subsequently

Mode 2 - 8.168 Hz

Mode 4 - 8.672 Hz

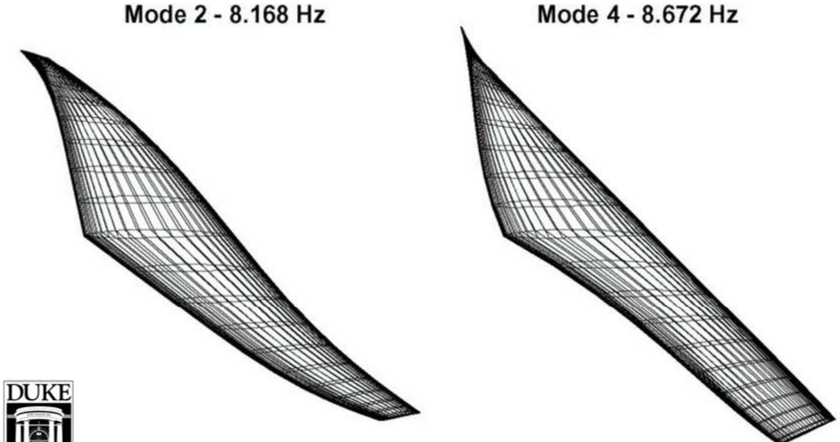

- FIGURE 12

Computed F-16 Flutter Onset Altitude Versus Mach Number Trend

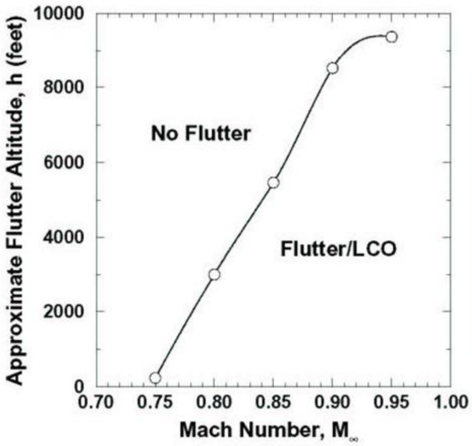

Mach Number	Altitude (feet)	Freq. (Hz)	ξ_4/ξ_2
0.75	228	8.55	(2.55 ,-6.46)
0.80	3093	8.55	(2.05 ,-6.37)
0.85	5630	8.54	(1.22 ,-6.05)
0.90	8440	8.54	(0.236,-4.55)
0.95	9388	8.53	(0.589,-2.81)

- FIGURE 13 **F-16 FLUTTER BOUNDARY**

F-16

FIGURE 14: F-16 (Block 40) Experimental LCO Aircraft Weapons and Stores Configurations

Stn.	Configuration 1	Configuration 2	Configuration 3
1	LAU-129 launcher	AIM-9L missile/LAU-129 launcher	LAU-129 launcher
2	AIM-9P missile/LAU-129 launcher	AIM-9L missile/LAU-129 launcher	AIM-120 missile/LAU-129 launcher
3	Air-to-ground missile	Air-to-ground missile	General purpose bomb
4	Empty 370-gal fuel tank	Half-full 370-gal fuel tank	Quarter-full 370-gal fuel tank
5	Empty station	Empty station	Empty station
6	Empty 370-gal fuel tank	Half-full 370-gal fuel tank	Quarter-full 370-gal fuel tank
7	Air-to-ground missile	Air-to-ground missile	General purpose bomb
8	AIM-9P missile/LAU-129 launcher	AIM-9L missile/LAU-129 launcher	AIM-120 missile/LAU-129 launcher
9	LAU-129 launcher	AIM-9L missile/LAU-129 launcher	LAU-129 launcher

FIGURE 15: F-16C Configuration Natural Frequencies

Mode	Configuration 1	Configuration 2	Configuration 3
First Bending (f_{1ab})	8.17 Hz	5.47 Hz	6.50 Hz
First Twisting (f_{1at})	8.67 Hz	5.74 Hz	7.32 Hz
Second Bending (f_{2ab})	10.9 Hz	7.87 Hz	8.37 Hz
Second Twisting (f_{2at})	12.3 Hz	8.01 Hz	8.97 Hz
$f_{1at} - f_{1ab}$	0.504 Hz	0.265 Hz	0.820 Hz

Antisymmetric Modes Via NASTRAN

FIGURE 16: LCO Response vs Mach Number: Sensitivity to Uncertainty in Aerodynamic Modeling of Tip Missile and Structural Natural Frequencies

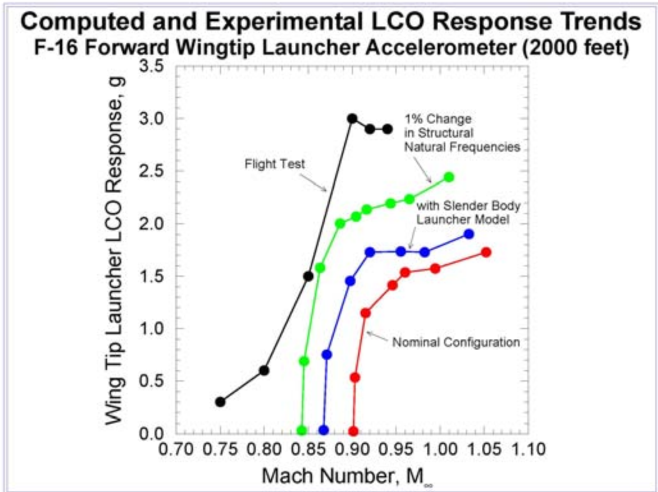

FIGURE 17: F-16 Flight Test Wingtip LCO Response

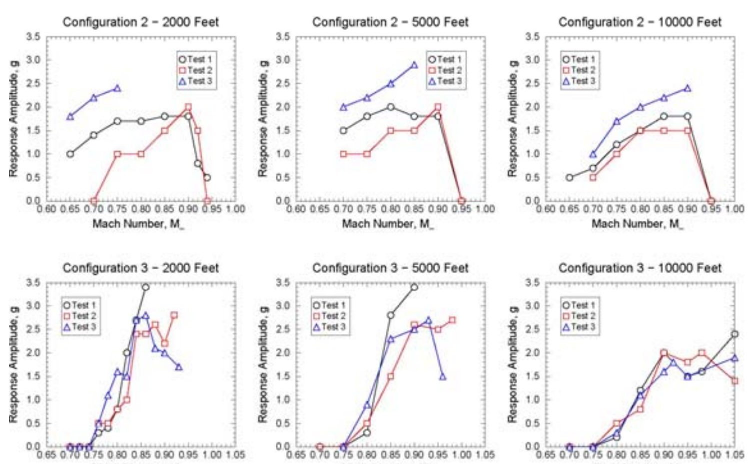

STRUCTURAL NATURAL FREQUENCY EFFECT ON FLUTTER BOUNDARY: ALTITUDE VERSUS MACH NUMBER

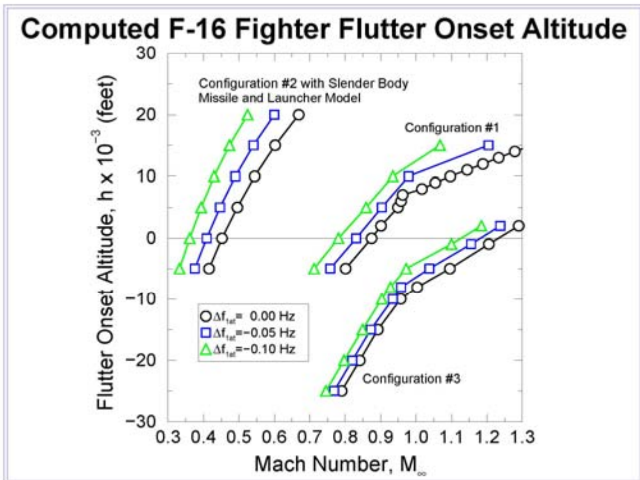

FIGURE 18: Flutter Onset Altitude vs Mach Number

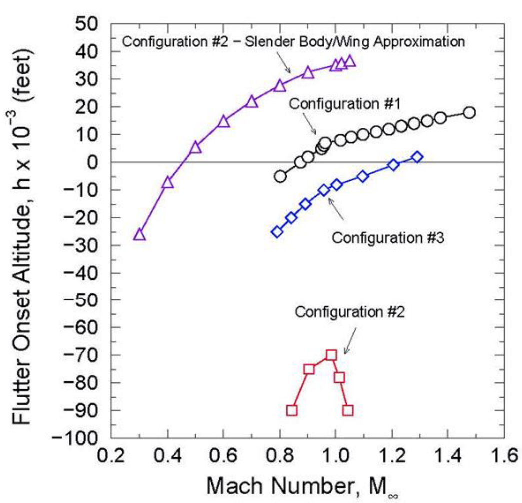

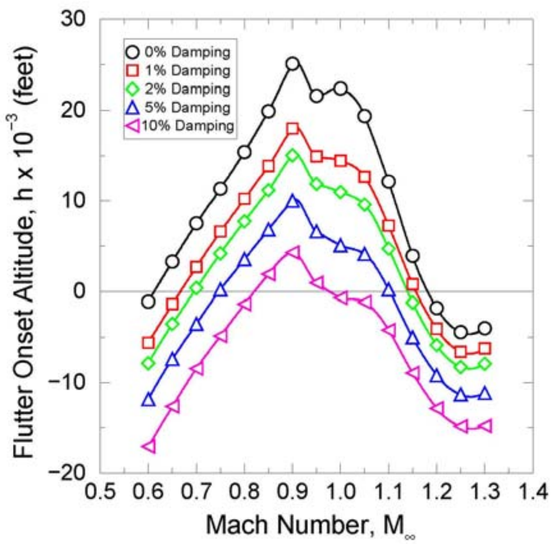

Figure 1: Computed F-16 Configuration Configuration # 5 Flutter Onset Trends for Different Levels of Structural Damping.

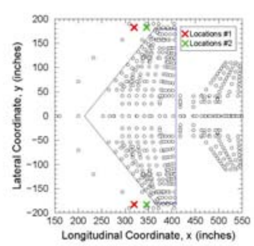

Figure 1: F-16 Configuration Number Five Structural Model Computational Nodes with Added Mass Locations Indicated.

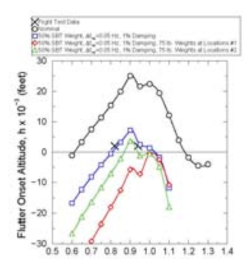

Figure 2: Sensitivity of Computed Flutter Onset for F-16 Configuration Number Five with 75 Pounds of Added Mass to Wingtip Launchers at Two Different Locations

FLUTTER VELOCITY VS. FOLDING ANGLE

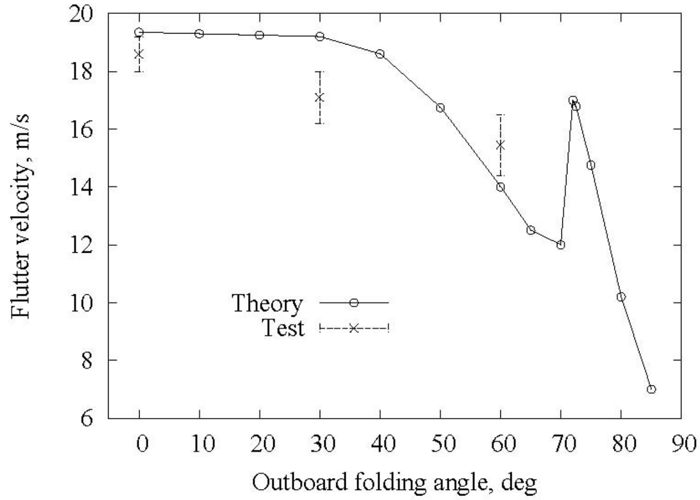

- FIGURE 19 **FOLDING WING FLUTTER BOUNDARY**

FLUTTER FREQUENCY VS. FOLDING ANGLE

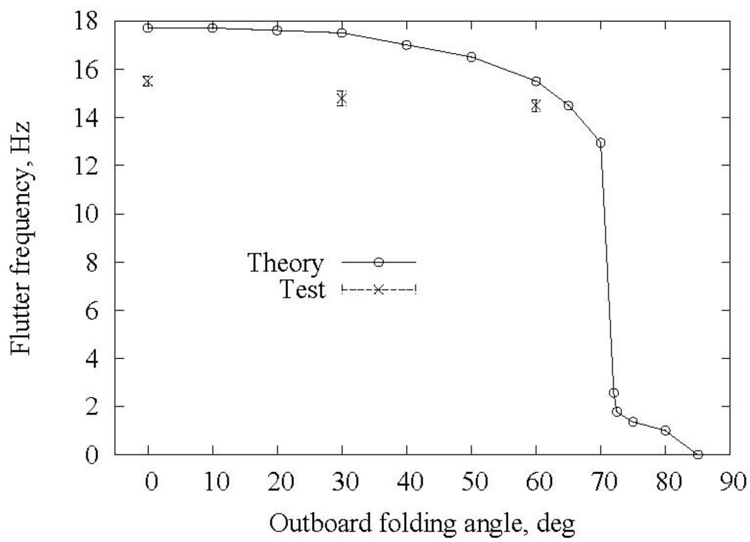

- FIGURE 20 **FLUTTER FREQUENCY**

ACCURATE, EFFECTIVE AND EFFICIENT COMPUTATIONAL METHODS: THREE IMPORTANT IDEAS

1. FIRST DETERMINE A NONLINEAR STATIC STATE OF THE SYSTEM, THEN CONSIDER SMALL (LINEAR) DYNAMIC PERTURBATION ABOUT THAT STATIC STATE, E.G. A NONLINEAR STEADY FLOW WITH SHOCKS AND/OR FLOW SEPARATION. THE "LOCAL" (IN PHASE SPACE) SYSTEM STABILITY MAY THEN BE DETERMINED.

2. FOR A NONLINEAR, DYNAMIC MODEL EXPAND THE SOLUTION IN A FOURIER SERIES IN TIME AND RETAIN ONLY A FEW HARMONICS. THIS IS NORMALLY SUFFICIENT TO DETERMINE LIMIT CYCLE OSCILLATIONS OF FLUID-STRUCTURAL SYSTEMS.

3. EXPAND SOLUTION IN TERMS OF GLOBAL MODES FOR STRUCTURE AND FLUID.

- COMPUTATIONAL COST OF (1) OR (2) IS COMPARABLE TO THAT OF THE NONLINEAR STATIC OR STEADY FLOW SOLUTION
- COMPUTATIONAL COST OF (3) IS USUALLY REDUCED BY SEVERAL ORDERS OF MAGNITUDE OVER THAT OF A SOLUTION BASED UPON A MODEL USING GENERALIZED COORDINATES ON LOCAL SPATIAL GRIDS

DUKE
EDMUND T. PRATT, JR. SCHOOL OF ENGINEERING

Aeroelastic Theoretical Model

- **Governing Equations:** $\mathcal{M}\left(-\omega^2 \mathrm{I} + \Omega^2\right)\xi - \mathcal{Q} = 0$
- **Structural Portion:**

$$\mathcal{M}\left(-\omega^2 \mathrm{I} + \Omega^2\right)\xi$$

  - Linear Reduced Order Modal Structural Modal.
  - Based on Modes Shapes from NASTRAN.

- **Fluid Dynamic Portion:**

$$\mathcal{Q} = \mathcal{Q}(\omega, \xi, M_\infty, \bar{\alpha}_0, h) = -\iint_A \bar{p}_1 \, \phi_{z_m} n_z \, \mathrm{dA}$$

  - Nonlinear Function of Displacement Amplitude ξ.
  - Based on Unsteady Pressure $\bar{p}_1$ (Frequency Domain) from Harmonic Balance/CFD Method.

DUKE
EDMUND T. PRATT, JR. SCHOOL OF ENGINEERING

Harmonic Balance (HB) Method

- Start With Unsteady Time-Domain CFD Method:

$$\frac{d\mathrm{Q}}{dt} + \mathrm{N}(\mathrm{Q}) = 0$$

- Fourier Series Expansion:

$$\mathrm{Q}(\mathrm{x}, t) \approx \sum_{n=-N}^{N} \hat{\mathrm{Q}}_n(\mathrm{x}) e^{jn\omega t} \quad \text{and} \quad \mathrm{N}(\mathrm{x}, t) \approx \sum_{n=-N}^{N} \hat{\mathrm{N}}_n(\mathrm{x}) e^{jn\omega t}$$

- Revert Back to Time (Discrete Subtime Levels) Domain Variables

$$\hat{\mathrm{Q}}_{-2}, \hat{\mathrm{Q}}_{-1}, \hat{\mathrm{Q}}_0, \hat{\mathrm{Q}}_1, \hat{\mathrm{Q}}_2 \Longleftrightarrow \mathrm{Q}(t_0+\Delta t), \mathrm{Q}(t_0+2\Delta t), \mathrm{Q}(t_0+3\Delta t), \mathrm{Q}(t_0+4\Delta t), \mathrm{Q}(t_0+5\Delta t)$$

$$\hat{\mathrm{N}}_{-2}, \hat{\mathrm{N}}_{-1}, \hat{\mathrm{N}}_0, \hat{\mathrm{N}}_1, \hat{\mathrm{N}}_2 \Longleftrightarrow \mathrm{N}(t_0+\Delta t), \mathrm{N}(t_0+2\Delta t), \mathrm{N}(t_0+3\Delta t), \mathrm{N}(t_0+4\Delta t), \mathrm{N}(t_0+5\Delta t)$$

- Harmonic Balance System

$$\underbrace{\omega \begin{bmatrix} & \mathrm{D} & \end{bmatrix}}_{\omega \begin{bmatrix} \mathrm{E}^{-1} \end{bmatrix} \begin{bmatrix} -jN & & \\ & \ddots & \\ & & jN \end{bmatrix} \begin{bmatrix} \mathrm{E} \end{bmatrix}} \begin{Bmatrix} \mathrm{Q}(t_0) \\ \mathrm{Q}(t_0+\Delta t) \\ \vdots \\ \mathrm{Q}(t_0+2N\Delta t) \end{Bmatrix} + \begin{Bmatrix} \mathrm{N}(t_0) \\ \mathrm{N}(t_0+\Delta t) \\ \vdots \\ \mathrm{N}(t_0+2N\Delta t) \end{Bmatrix} = \begin{Bmatrix} 0 \\ 0 \\ \vdots \\ 0 \end{Bmatrix}$$

- Pseudo March to Steady State

DUKE
EDMUND T. PRATT, JR.
SCHOOL OF ENGINEERING

HB Methodology Continued

Easy To Implement Within Existing STEADY Flow Solver.

- Re-dimension Primary Arrays by $(2N+1)$.
- Add Source Term DU to Algorithm.

Steady Flow Solution Acceleration Techniques Can Be Used to Accelerate Harmonic Balance Solution.

- Local Time-Stepping, Preconditioning, Multi-grid, etc.

Computational Cost Behaves as $\mathcal{O}(2N+1)$ Times the Cost of a Single STEADY Flow Solution.

Three Different Flow Solvers All Contained in One Code.

- Steady Flow Solver.
- Linear Unsteady Solver.
- Non-linear Unsteady Solver.

DUKE
EDMUND T. PRATT, JR.
SCHOOL OF ENGINEERING

Details of F-16 HB/CFD Model

- Reynolds Averaged Navier (RANS) Stokes CFD Model.
- Modified Lax-Wendroff CFD Method.
- Spalart and Allmaras Turbulence Model.
- 65 x 33 x 49 Mesh - 105,105 Nodes - 630,630 DOF.
- Standard Atmosphere Conditions Considered.
- For Mach Numbers and Altitudes Studied,
  $80 \times 10^6 \leq Re_{\infty_{cr}} \leq 120 \times 10^6$.
- Constant Mean Angle of Attack, $\bar{\alpha}_0 = 1.5$ (deg)

Linear Aeroelastic Theoretical Model to Establish Flutter Onset Conditions

- Governing Equation:
  $$\left[\mathcal{M}(-\omega^2 \mathbf{I} + \Omega^2) - \frac{\partial \mathcal{Q}}{\partial \xi}\right] \xi = 0$$
- Linearized Aerodynamics: $\frac{\partial \mathcal{Q}}{\partial \xi}$
  - ▷ Solution Snapshots for Discrete Frequencies and Motions ξ.
  - ▷ Compute Using HB Solver Run for Very Small Amplitude Motions.
- Equation Above Is An Eigenvalue Problem: $[\mathrm{G}(h, \omega)]\, \xi = 0$
  - ▷ The Combination of (h, ω) where $|\mathrm{G}(h, \omega)| = 0$ Establishes Flutter Onset Condition.
  - ▷ Also Provides Initial Condition for LCO Solver.

HB/LCO Aeroelastic Solution Methodology

- Governing Equations:

$$\mathcal{M}(-\omega^2 \mathrm{I} + \Omega^2)\frac{\xi}{\xi_a} - \frac{\mathcal{Q}}{\xi_a} = 0$$

- Real and Imaginary Parts Represent Nonlinear Vector Equation:

$$\mathrm{R}(\mathrm{L}, \xi_a) = 0 \quad \text{where} \quad \mathrm{L} = \begin{Bmatrix} M_\infty \\ \omega \\ \mathrm{Re}(\xi_b)/\xi_a \\ \mathrm{Im}(\xi_b)/\xi_a \\ \vdots \end{Bmatrix}$$

- Use Newton-Raphson Technique to Solve for L

$$\mathrm{L}^{n+1} = \mathrm{L}^n - \left[\frac{\partial \mathrm{R}(\mathrm{L}^n)}{\partial \mathrm{L}}\right]^{-1} \mathrm{R}(\mathrm{L}^n)$$

DUKE
EDMUND T. PRATT, JR.
SCHOOL OF ENGINEERING

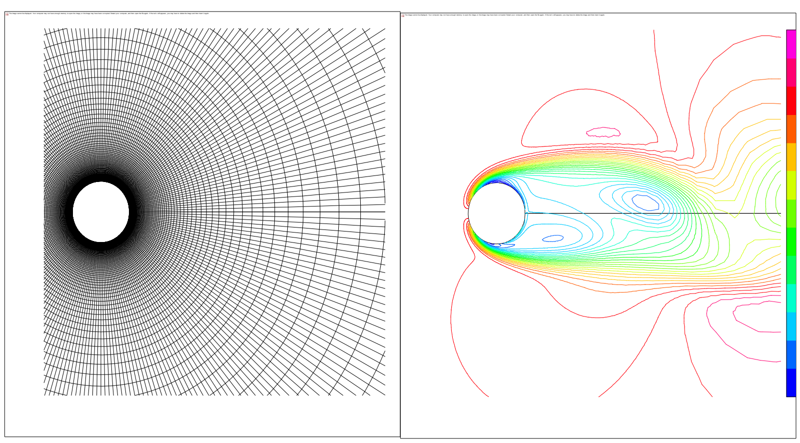

UNSTEADY VORTEX SHEDDING AFT OF A CYLINDER IN CROSSFLOW, RE=150.

DUKE
EDMUND T. PRATT, JR.
SCHOOL OF ENGINEERING

MAGNITUDE OF UNSTEADY LIFT AS A FUNCTION OF REYNOLDS NUMBER.

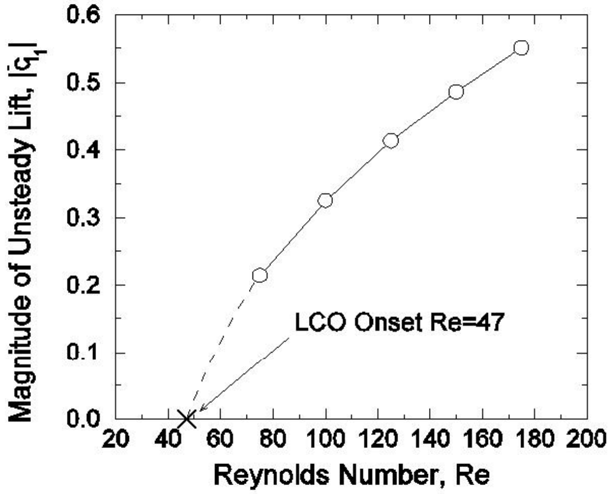

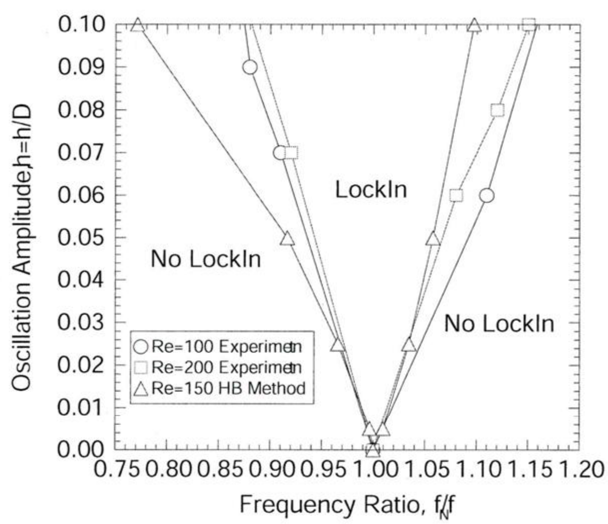

Oscillation Amplitude vs. Ratio of Strouhal Frequency of Wake to Prescribed Frequency of Cylinder Motion

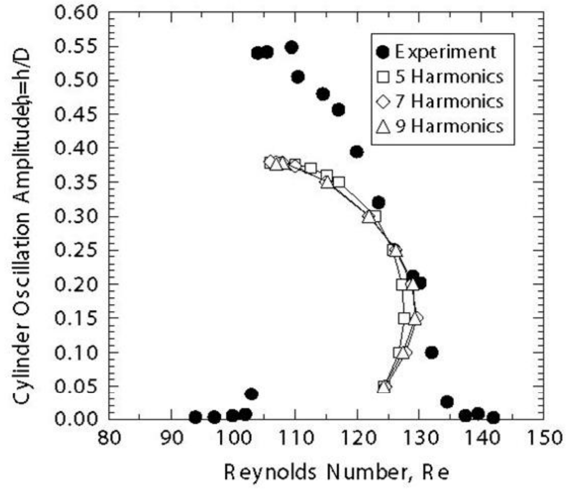

LCO Amplitude versus Reynolds Number

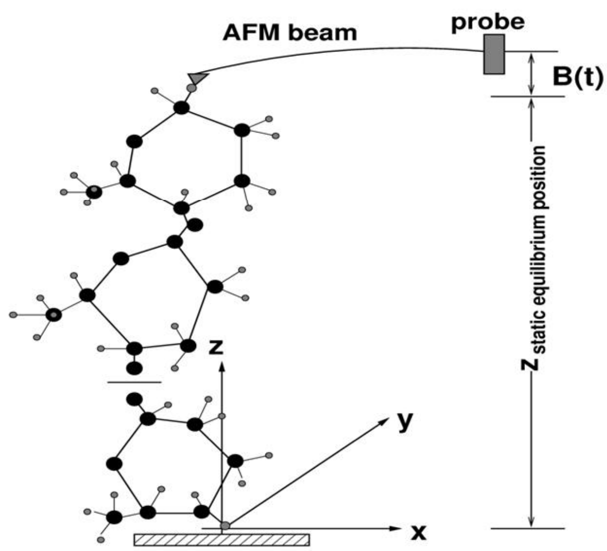

Schematic Diagram for Stretching of the Molecule by an AFM

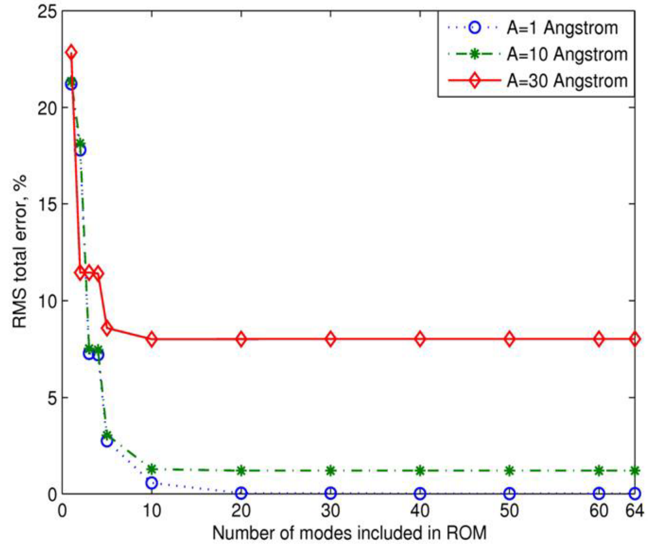

Total RMS Error vs. Number of Eigenmodes for Different Excitation Amplitudes Using the Linear ROM f=100GHz

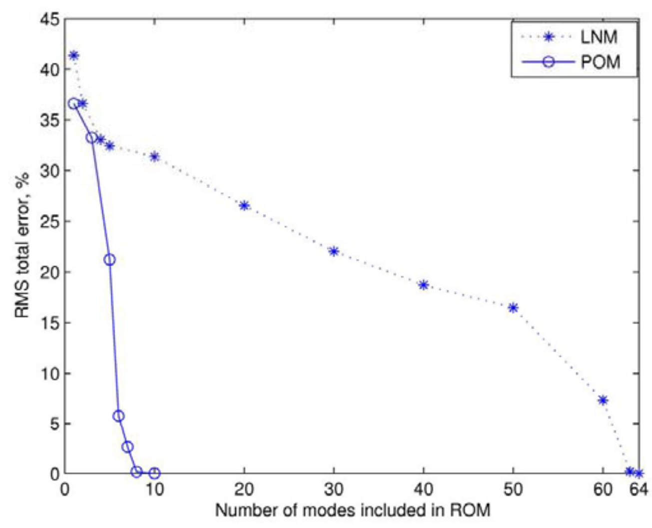

Total RMS Error vs. Number of LNM or POM Included in the Nonlinear ROM. A=1Å and f=100GHz

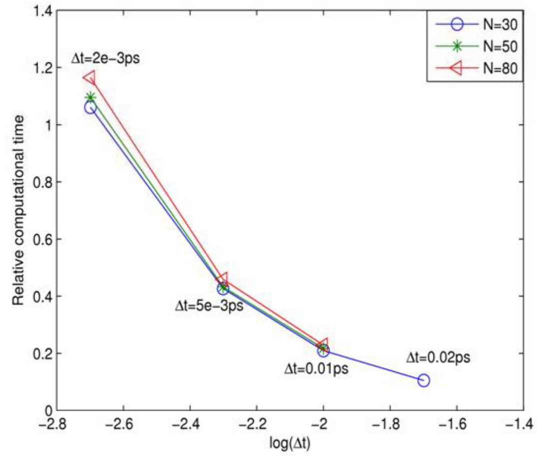

Ratio of Computational Time for ROM (POD and CMS) model to that of a Time Marching Solution Vs. the Chosen Numerical Time Step for Different Number of Modal Coordinates retained, N, in the whole system. A=Å and f=20GHz

CONCLUSIONS

- A COMBINATION OF OLD AND NEW METHODS CAN GREATLY REDUCE THE SIZE OF MATHEMATICAL MODELS AND INCREASE THE SPEED OF THEIR SIMULATION

- THESE METHODS INCLUDE:
  - HARMONIC BALANCE SOLUTIONS
  - GLOBAL FLUID MODAL REPRESENTATION
  - DYNAMIC LINEARIZATION ABOUT NONLINEAR STATIC EQUILIBRIA

- CORRELATIONS OF LCO COMPUTATIONS AND TESTS ARE ENCOURAGING, BUT MUCH WORK REMAINS TO BE DONE